

# 40-Gb/s Tandem Electroabsorption Modulator

Beck Mason, Abdallah Ougazzaden, Charles W. Lentz, Kenneth G. Glogovsky, C. Lewis Reynolds, George J. Przybylek, Ronald E. Leibenguth, Terry L. Kercher, John W. Boardman, Michael T. Rader, J. Michael Geary, Frank S. Walters, Larry J. Peticolas, Joseph M. Freund, S. N. George Chu, Andrei Sirenko, Ronald J. Jurchenko, Mark S. Hybertsen, Leonard J. P. Ketelsen, and Greg Raybon

**Abstract**—In this letter, we have developed a tandem electroabsorption modulator with an integrated semiconductor optical amplifier that is capable of both nonreturn-to-zero and return-to-zero (RZ) data transmission at 40 Gb/s. The tandem modulator consists of a broad-band data encoder and a narrow-band pulse carver. The pulse carver is able to produce 5-ps pulses with more than 20 dB of extinction. The on-chip semiconductor optical amplifier provides up to 8.5 dB of fiber-to-fiber gain and enables the modulator to be operated with zero insertion loss. Devices have been realized with greater than 40-GHz bandwidth, and 13-dB dynamic extinction for a 2.5-V swing. For optimized designs bandwidths of nearly 60 GHz have been realized. Using these devices penalty free RZ data transmission over a 100-km dispersion compensated fiber link has been demonstrated with a received power sensitivity of  $-29$  dBm.

**Index Terms**—Electroabsorption modulators, semiconductor optical amplifiers.

## I. INTRODUCTION

ELECTROABSORPTION modulated sources are key components for current and next generation 40-Gb/s fiber transport systems. Electroabsorption modulators (EAMs) offer advantages in compactness, low cost, compatibility with monolithic integration, and low drive voltages. In this letter, we describe the design, fabrication, and transmission performance of 40-Gb/s tandem EA modulators capable of both nonreturn-to-zero (NRZ) and return-to-zero (RZ) operation. The device structure consists of two short multiple-quantum-well (MQW) modulators, a monolithically integrated semiconductor optical amplifier (SOA), and spot-size converters (SSCs) on both the input and output. For RZ transmission, one modulator functions as a pulse carver, and the other one operates as a data encoder. For NRZ operation, the pulse carver is not used. The tandem modulator design was realized using semi-insulating InP regrown deep ridge buried heterostructure technology. Modulation bandwidths of up to 57 GHz have been demonstrated for the smallest device geometries. The carver/encoder configuration with the SOA operates with up to 8.5-dB fiber-to-fiber gain at a 0-V modulator bias. This device is intended for long-haul RZ data transmission.

There are significant advantages to using short pulse RZ transmission for long distance 40-Gb/s communications

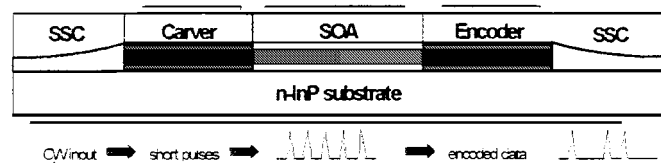


Fig. 1. Tandem modulator cross section.

systems [1]. For these systems, a transmitter is required that can generate short optical pulses and encode them using data modulation. A semiconductor-based tandem electroabsorption modulator (TEAM) offers a single compact device incorporating both stable short pulse generation and data modulation functions. The first demonstration of a TEAM was at 5 Gb/s using two discrete InGaAsP bulk modulators [2]. Fiber-to-fiber insertion loss resulting from the two components was 15 dB. To reduce the optical losses, tandem modulators integrated with optical amplifiers have been reported. As a result, tandem device fiber-to-fiber insertion loss was reduced to 9 dB, and operation at 20 Gb/s was demonstrated [3]. In this letter, we report on a TEAM with better than 0-dB insertion loss and greater than 40-GHz bandwidth.

## II. DEVICE DESIGN

The tandem modulator consists of a semiconductor optical amplifier sandwiched between two EAMs (see Fig. 1). Spot size converters are used on the input and output waveguide to improve the optical coupling efficiency. The modulators and the SOA have a MQW active layer with a thin separate confinement heterostructure. The device is fabricated using a deep ridge buried heterostructure process.

Modulators with varying lengths of 80, 100, and 120  $\mu\text{m}$  were evaluated with SOA lengths of 400 and 600  $\mu\text{m}$ . In this letter, we show results for two different modulator active layer designs. The first structure (Type I) has a 0.2- $\mu\text{m}$ -thick depletion region. In the second structure (Type II), we increased the depletion region thickness to 0.3  $\mu\text{m}$ . These two structures were designed to investigate the tradeoff between the bandwidth and the extinction ratio for EAMs of varying lengths. Type I devices have a narrow depletion region which maximizes the internal field, and thus, the change in absorption for a given drive voltage. Type II devices have a wider depletion region giving them a smaller junction capacitance, which will result in a higher bandwidth for a given device length, assuming that the radiatively coupled (RC) bandwidth limit due to the junction capacitance dominates over the parasitic effects.

Manuscript received June 25, 2001; revised August 9, 2001.

B. Mason, A. Ougazzaden, C. W. Lentz, K. G. Glogovsky, C. L. Reynolds, G. J. Przybylek, R. E. Leibenguth, T. L. Kercher, J. W. Boardman, M. T. Rader, J. M. Geary, F. S. Walters, L. J. Peticolas, J. M. Freund, S. N. G. Chu, A. Sirenko, R. J. Jurchenko, M. S. Hybertsen, and L. J. P. Ketelsen are with Agere Systems, Breinigsville, PA 18031 USA.

G. Raybon is with Lucent Technologies, Holmdel, NJ 07733 USA.

Publisher Item Identifier S 1041-1135(02)00017-4.

### III. FABRICATION PROCEDURE

The TEAM-SOA-SSC structure shown in Fig. 1 is fabricated using four low pressure organometallic vapor phase epitaxy (LP-OMVPE) growths. First, the MQW active region of the two modulators and SOA are formed using selective area growth on a mask patterned substrate. The composition and thickness of wells and barriers have been optimized for high extinction ratio and low modulator chirp. Spot size converters are connected to the modulators by precise dry etching of the active region, followed by selective area growth (SAG) assisted butt-joint regrowth of passive waveguides. The SAG growth produces an adiabatic vertical waveguide taper along the length of the spot size converter. Reduced waveguide thickness at the device input and output facets provides good coupling to lensed optical fiber, while a thicker waveguide at the butt-joint yields good mode matching between the spot size converter and the modulator. In the third step, the waveguides are buried under a thick p-InP cladding layer and thin InGaAs contact layer. Narrow mesa stripes are then patterned using conventional photolithography and transferred to a SiO<sub>2</sub> etch mask. The deep ridge mesa's fabricated in the [011] direction are formed in an inductively coupled plasma (ICP) etching system. The ICP etching conditions were optimized for mesas with sharply defined vertical sidewalls and smooth morphology. Following this, the mesas were imbedded in Fe-doped semi-insulating InP. LP-OMVPE conditions were optimized for planar regrowth around the deep and narrow dry-etched mesas without the need for growth mask overhang. A thick spin on dielectric was then applied to reduce the parasitic capacitance of the p contact pads, which were designed to facilitate flip chip mounting of the device.

### IV. DEVICE PERFORMANCE

Using a tunable external cavity laser, and lensed fiber-coupling optics, the extinction ratio and insertion loss were measured for both single modulators without an SOA and tandem devices. Measured on-state insertion loss for single devices was as low as 6 dB. Tandem devices with 600- $\mu\text{m}$ -long SOAs, displayed up to 8.5-dB fiber-to-fiber gain with 150-mA SOA drive current, 0-V bias on the modulators, and 0-dBm input power. With both modulators at 0-V 0-dB insertion loss was achieved with as little as 50-mA SOA current. The frequency response for the modulators was measured using a 50-GHz vector network analyzer and a calibrated photodiode (Fig. 2). For Type I devices the 3-dB bandwidths for the 80- and 120- $\mu\text{m}$ -long modulators were 38 and 30 GHz, respectively. For Type II devices the bandwidth for the 120- $\mu\text{m}$ -long modulator was 39 GHz and for the 80- $\mu\text{m}$ -long modulator it was estimated to be 57 GHz based on a fit to the data measured out to 50 GHz.

The tradeoff for this improved bandwidth in the Type II devices is a reduction in the slope of the extinction curves. However, for the same bandwidth of 40 GHz, we can use a modulator that is 50% longer with a Type II structure than we can with a Type I structure. Fig. 3 shows a comparison of the extinction curves for an 80- $\mu\text{m}$ -long Type I modulator and a 120- $\mu\text{m}$ -long Type II modulator, both devices have approximately 40-GHz bandwidths.

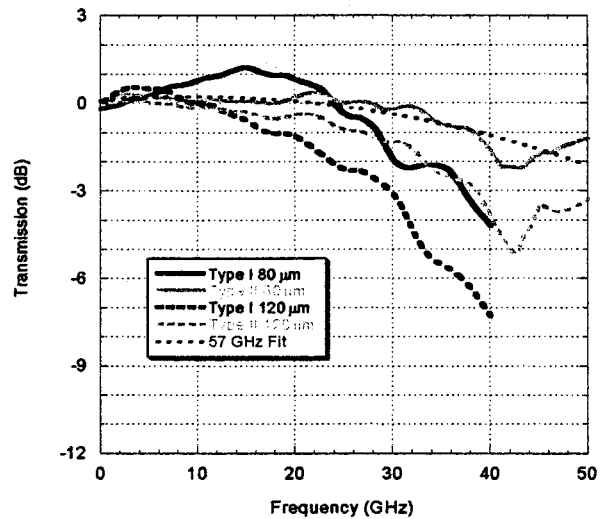


Fig. 2. Modulator bandwidth comparison.

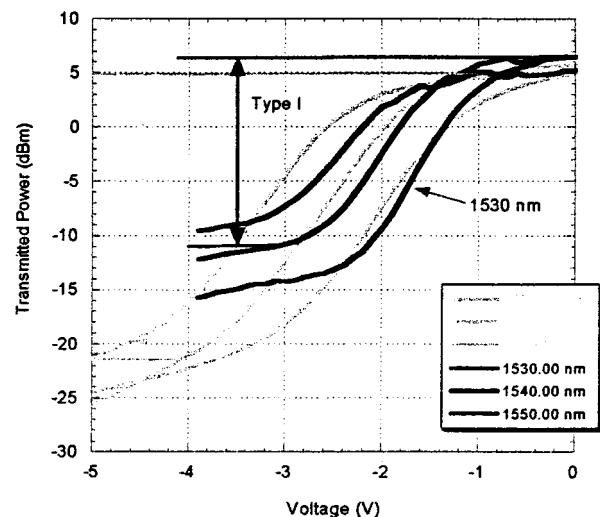


Fig. 3. The dc extinction ratio curves for Type I and Type II modulators at various wavelengths.

For a 3-V swing at 1540 nm the Type I device has a dc extinction ratio of 18.5 dB, whereas the Type II device has a dc extinction ratio of 26 dB. For lower voltage operation it might be expected that the Type I would have better performance however for a 2-V swing the Type II device still has a 4 dB greater extinction ratio.

Using a tandem modulator, we can produce both 40-Gb/s NRZ (Fig. 4) and 40-Gb/s RZ (Fig. 5) data transmission. Both eye diagrams were measured using a 34-GHz bandwidth photodiode with a 50-GHz bandwidth sampling scope. Input power from an external cavity tunable laser was set at +6 dBm and the on-chip SOA was biased at 80 mA. The NRZ pattern was produced by directly driving the data encoder with the 2.5-Vpp output from an SHF (SHF Communication Technologies AG) 40-Gb/s pattern generator using a 2<sup>31</sup>-1 word length. The rise and fall times for the electrical signal were 18 ps. For 40-Gb/s NRZ transmission an open eye is observed in the presence of up to 60 ps/nm total dispersion. The RZ eye was generated by driving the SHF from an external 20-GHz clock source. This external clock was doubled to 40 GHz and then amplified to drive

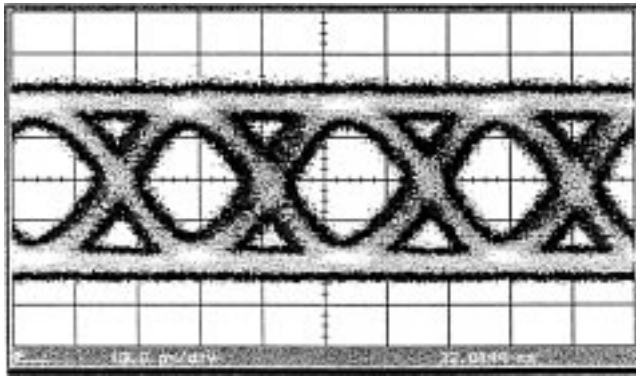


Fig. 4. 40-Gb/s NRZ eye diagram for Type II modulator measured at 3-dBm output power.

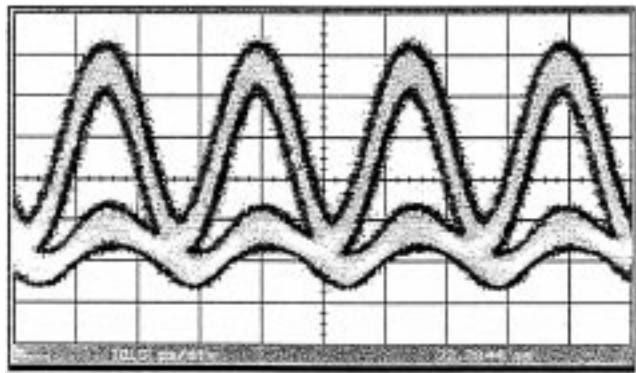


Fig. 5. 40-Gb/s RZ eye diagram for Type II modulator measured at 3-dBm output power.

the pulse carver. A trombone phase shifter was used to align the pulse carver and data encoder drive signals.

Streak camera measurements revealed pulsewidths of 7-ps and 20-dB extinction ratio for a 40-GHz 5-Vpp narrow-band drive signal. Pulsewidths as short as 5 ps were achieved at higher drive voltages. Using this device 40-Gb/s RZ transmission experiments were conducted using a 10-Gb/s BERT with a  $4 \times 1$  electronic multiplexer and an optical demultiplexer. The back-to-back receiver sensitivity was  $-29$  dBm, and a negligible transmission penalty was obtained over a 100-km dispersion compensated link (Fig. 6), consisting of a launch erbium-doped fiber amplifier (EDFA), 100 km of TrueWave fiber, followed by a backward pumped Raman amplifier, and a section of dispersion compensating fiber. An EDFA was used to boost the launch power to 6 dBm. The extremely low observed penalty suggests that transmission can be achieved over considerably longer distances. Excellent NRZ and RZ

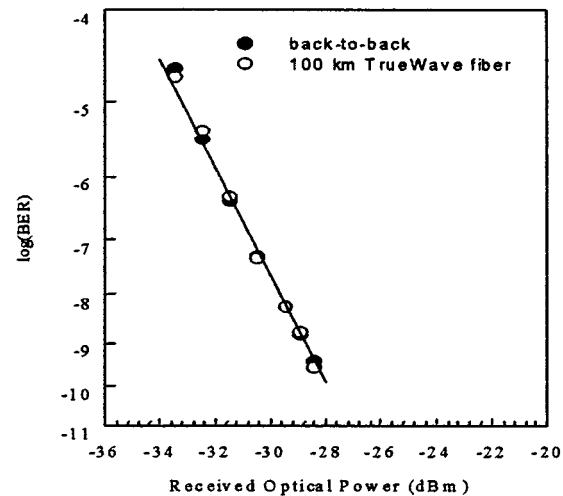


Fig. 6. BER measurement with Type I device.

results also confirm the high bandwidth, high extinction, and low-chirp characteristics of this device.

## V. CONCLUSION

Using a SI-InP regrown deep ridge buried heterostructure, we have fabricated the first 40-Gb/s TEAM with integrated semiconductor optical amplifier and input/output spot-size converters. Zero insertion loss, high dynamic extinction ratio, 40-GHz bandwidth, and 7-ps pulse generation were simultaneously demonstrated. Over standard single-mode fiber, 40-Gb/s NRZ transmission was achieved in the presence of 60-ps/nm chromatic dispersion. With a 100-km dispersion managed link, error-free 40-Gb/s RZ data transmission was demonstrated using carver/encoder operation. The low chirp, wide bandwidth, and good extinction ratio of this device demonstrate its utility in both short reach and long-haul 40-Gb/s applications.

## REFERENCES

- [1] R.-J. Essiambre, B. Mikkelsen, and G. Raybon, "Intra-channel cross-phase modulation and four-wave mixing in high-speed TDM systems," *Electron. Lett.*, vol. 35, no. 18, pp. 1576–1578, 1999.
- [2] H. Tanaka, S. Takagi, M. Suzuki, and Y. Matsushima, "Optical short pulse generation and data modulation by a single-chip InGaAsP tandem-integrated electroabsorption modulator (TEAM)," *Electron. Lett.*, vol. 29, no. 11, pp. 1002–1004, 1993.
- [3] N. Souli, F. Devaux, A. Ramdane, Ph. Krauz, A. Ougazzaden, F. Huet, M. Carre, Y. Sorel, J. F. Kerdiles, M. Henry, G. Aubin, E. Jeanney, T. Montallan, J. Moulu, B. Nortier, and J. B. Thomine, "20 Gbit/s high-performance integrated MQW TANDEM modulators and amplifier for soliton generation and coding," *IEEE Photon. Technol. Lett.*, vol. 7, pp. 629–631, June 1995.